



Methane emission of a lake aquaculture farm and its response to ecological restoration

Yini Pu^a, Mi Zhang^{a,b,*}, Lei Jia^a, Zhen Zhang^{a,c}, Wei Xiao^{a,b}, Shoudong Liu^a, Jiayu Zhao^a, Yanhong Xie^a, Xuhui Lee^{d,**}

^a Yale-NUIST Center on Atmospheric Environment, International Joint Laboratory on Climate and Environment Change (ILCEC), Nanjing University of Information Science and Technology, Nanjing, Jiangsu Province, China

^b Key Laboratory of Meteorological Disaster, Ministry of Education and Collaborative Innovation Center on Forecast and Evaluation of Meteorological Disasters, Nanjing University of Information Science and Technology, Nanjing, Jiangsu Province, China

^c Nanjing Jiangning District Meteorological Bureau, Nanjing, Jiangsu Province, China

^d School of the Environment, Yale University, New Haven, CT, USA

ARTICLE INFO

Keywords:

Subtropical lake
CH₄ flux
Enclosure aquaculture
Ecological restoration

ABSTRACT

Enclosure lake aquaculture causes lake eutrophication and emits CH₄ to the atmosphere. So far, little is known about the rate of CH₄ emission from lake aquaculture and about how ecological restoration (or aquaculture abandonment) affects the emission. In this study, the eddy covariance (EC) technique was deployed to quantify the CH₄ flux in an enclosure lake aquaculture farm and to investigate the flux response to ecological restoration. The lake site under aquaculture farming emitted 36.0 g C-CH₄ m⁻² yr⁻¹ to the atmosphere, an amount that is comparable to the global mean value of semi-intensive aquaculture systems. The annual CH₄ emission decreased from the pre-restoration level by 34% and 37% to 23.7 and 22.8 g C-CH₄ m⁻² yr⁻¹ in the first and second year of ecological restoration, respectively, but was still much higher than that at a reference lake site not impacted by aquaculture farming (6.12 g C-CH₄ m⁻² yr⁻¹). The high emission values after aquaculture abandonment suggest that aquafeed input in the decades of farming may have caused accumulation of a large amount of organic carbon in the sediment that continues to fuel CH₄ production and that it may take a long time for the system to recover to a natural state. After aquaculture abandonment, floating-leaved plants expanded rapidly within the EC flux footprint, resulting in a high net ecosystem productivity (NEP) in the growing season. These plants appeared to be able to transport CH₄ to the atmosphere through aerenchyma tissues and stomata.

1. Introduction

Freshwater aquaculture systems are a large source of CH₄ to the atmosphere, emitting more than 6 Tg CH₄ yr⁻¹ globally (Yuan et al., 2019). At present, pond aquaculture and lake aquaculture are the two main types of freshwater aquaculture (Bostock et al., 2010; Cowx and Ogotu-Owhayo, 2019). China's aquaculture sector is the largest in the world, accounting for more than 60% of global aquaculture production (FAO, 2020). Before 1980s, Chinese aquaculture was mainly carried out in earthen ponds. With the increasing demand for protein, intensive enclosure lake aquaculture has been widely practiced over the past 40 years (Wu et al., 2001; Jia et al., 2013), reaching the peak area of

approximately 1 million ha (China Fishery Statistical Yearbook, 2015).

As the name implies, farmers of enclosure aquaculture use seine nets and bamboo fences to enclose a section of a lake to raise fish (Xia et al., 2018; Dai et al., 2019). Generally, the selected areas are characterized by shallow depths (< 3 m), good water quality, and plentiful waterweeds. Different from pond aquaculture, water can flow in and out of the enclosure zone, and fish excreta is continuously diluted. A consequence of this water exchange is that the dissolved oxygen in the enclosure is relatively high, contributing to favorable growth conditions for aquatic animals (Xia et al., 2018; Yuan et al., 2019). During the aquaculture period, in addition to natural food provided by aquatic vegetation, farmers apply a large amount of artificial feed to pursue a high fish yield.

* Corresponding author at: Yale-NUIST Center on Atmospheric Environment, International Joint Laboratory on Climate and Environment Change (ILCEC), Nanjing University of Information Science and Technology, Nanjing, Jiangsu Province, China.

** Corresponding author.

E-mail addresses: zhangm.80@nuist.edu.cn (M. Zhang), xuhui.lee@yale.edu (X. Lee).

<https://doi.org/10.1016/j.agee.2022.107883>

Received 17 October 2021; Received in revised form 20 January 2022; Accepted 23 January 2022

Available online 2 February 2022

0167-8809/© 2022 Elsevier B.V. All rights reserved.

According to the data provided by the National Bureau of Statistics (2019), the mean feed consumed per season is estimated to be about 4600 kg (dry weight) ha⁻¹, equivalent to about 1500 kg C ha⁻¹. Fish yield from lake aquaculture ranges from 1040 to 1800 kg (wet weight) ha⁻¹ (China Fishery Statistical Yearbook, 2019).

Although enclosure aquaculture has brought economic returns, it has caused environmental problems. It is estimated that less than 9% of the nitrogen and less than 17% of the phosphorus in fish feed are consumed by fish (Wang et al., 2021). The majority of the nitrogen and phosphorus after decomposition are transported to the surrounding lake water, causing eutrophication and deterioration of water quality (Veenstra et al., 2003; Zeng et al., 2013; Wang et al., 2018). Another problem is concerned with loss of biodiversity and depletion of natural fishery resources resulting from intensive aquaculture (Rodríguez-Gallego et al., 2008; Xiao et al., 2010; De Silva, 2012). In order to restore the structure and function of lake ecosystems, the national and local governments in China have issued a series of regulations requiring that all enclosure farms be dismantled within a specified timeframe (Wang et al., 2015; Dai et al., 2019). According to China Fishery Statistical Yearbook (2019), the area of lake aquaculture decreased by approximately 25% from 2015 to 2019, and the decline will continue in the coming years.

The lake that undergoes ecological restoration will experience a number of changes from the perspective of methane emission. Firstly, prior to restoration, the existence of seine net reduces water flow, attenuates wind speed, and weakens the shear stress at the bottom of the lake. After net removal, the bottom shear stress tends to increase, which may trigger CH₄ ebullition (Joyce and Jewell, 2003; Taoka et al., 2020). Ebullition allows CH₄ to escape oxidation in the water column, thus increasing the total CH₄ emission at the water-air interface (Jeffrey et al., 2019; Iwata et al., 2020). Secondly, without allochthonous carbon input via fish feed, the organic substrate available for lake CH₄ production is reduced (Bastviken et al., 2004; Grasset et al., 2018). Thirdly, without human interference, aquatic vegetation tends to flourish, thus providing more autochthonous organic substrate for methanogenesis than prior to restoration (Laanbroek et al., 2010; Grasset et al., 2018). The importance of autochthonous organic substrate has been demonstrated by a study at Lake Taihu, where the CH₄ emission in a submerged aquatic vegetation zone is 3.5 times higher than that from a zone free of aquatic vegetation (Zhang et al., 2019). Fourthly, apart from biomass amount, aquatic vegetation type will also change. Floating-leaved plants, as the pioneer species, recover quickly after seine net removal (Wang et al., 2021). Floating plant leaves are likely to reduce ebullition by intercepting CH₄ bubbles (Kosten et al., 2016) but may simultaneously promote plant-mediated CH₄ transport through aerenchyma tissues and stomata (Bolpagni et al., 2007; Villa et al., 2020). So far, our understanding is poor regarding the net effect of these changes on the annual CH₄ emission.

Here, we hypothesize that the loss of allochthonous carbon input outweighs the role of increased in-situ productivity and that the CH₄ emission will decrease rapidly with time after the start of ecological restoration. We tested this hypothesis with eddy covariance (EC) observation in Lake Taihu, a shallow freshwater lake in China. The EC site was located in the eastern portion of the lake where submerged vegetation is abundant as a natural food source for aquatic animals and where the water quality is better than the western and northern portions of the lake impacted by urban and agricultural runoffs. This portion of the lake had been used for aquaculture since the 1980s until year 2018, the last year of aquaculture. A permanent ban of aquaculture in Lake Taihu has been enforced since the beginning of 2019.

To date, a large number of studies have been conducted on methane emission in fish ponds (Hu et al., 2016; Yang et al., 2018; Rutegwa et al., 2019; Yuan et al., 2019; Shafer et al., 2020; Zhao et al., 2021). In comparison, our understanding of methane emission in enclosure aquaculture is limited. Using floating chamber observations made on six days, da Silva et al. (2018) obtained a mean CH₄ flux density of 6.5 μg CH₄ m⁻² s⁻¹ for net cage aquaculture in a reservoir system. This flux

density is much greater than the mean value of rice paddies and is also greater than the flux density of most fish ponds (Zhao et al., 2021), suggesting that enclosure aquaculture may be an important source of atmospheric CH₄. But because of the limited temporal coverage of their study, it is not known whether their result can be extended to the whole year or to other enclosure aquaculture systems. Our study appears to be the first to report annual CH₄ emission from enclosure aquaculture.

The specific objectives of this study are (1) to quantify the annual CH₄ emission of the enclosure aquaculture farm in Lake Taihu, (2) to examine the temporal dynamics of CH₄ flux before and after seine net removal, (3) to investigate the impact of vegetation recovery on CH₄ emission pathways, and (4) to identify factors that control CH₄ flux over multi-temporal scales.

2. Material and methods

2.1. Site description

Lake Taihu is located in the Yangtze River Delta in Eastern China. It is the third largest freshwater lake in China, with an area of 2340 km² and an average depth of 1.9 m (Qin et al., 2007). Lake Taihu experiences a subtropical humid monsoon climate, with mean temperature, annual precipitation, and mean wind speed of 16.2 °C, 1122 mm, and 2.6 m s⁻¹, respectively (Lee et al., 2014). Inflow rivers are mainly distributed in the northern and western portions, while outflows are mostly located in the eastern portion, resulting in NW to SE spatial gradients of nutrient loadings. East Lake Taihu (area 131 km²) in the southeast corner of Lake Taihu is characterized by shallow water depths (< 1.5 m), abundant macrophytes, and good water quality (Zhao et al., 2017). The annual mean concentrations of total nitrogen and total phosphorus from 1985 to 2015 were 1.48 mg L⁻¹ and 0.053 mg L⁻¹, respectively (Dai et al., 2016). Enclosure aquaculture in East Lake Taihu began in 1984 and had expanded rapidly until 2018, reaching a peak total area of 106.5 km².

The aquaculture in East Lake Taihu employed a polyculture mode dominated by the Chinese mitten crab (*Eriocheir sinensis*) and supplemented by black shrimp (*Macrobrachium nipponense*) and giant river prawn (*Macrobrachium rosenbergii*). Before the aquaculture season, quicklime was used first to improve water quality. Young crab fry (about 10 g ind⁻¹) was stocked at the density of 15,000 ind ha⁻¹ in mid-January. Black shrimp fry (about 0.5 g ind⁻¹) and giant river prawn (about 12 g ind⁻¹) were stocked in March and June at the density of 225,000 and 12,000 ind ha⁻¹, respectively. Submerged plants, such as *Elodea nuttallii*, were vegetated in May to provide the crabs with shelter and food. Mature crabs and shrimps were harvested from mid-September to late December. Pellet feed, fish meat, and corn seed were applied once per day between 4:00 AM and 6:00 AM from mid-January to mid-October, and the daily application rate depended on the growth status of the aquatic animals. The annual applications were 640 kg C ha⁻¹ yr⁻¹ (pellet feed), 1580 kg C ha⁻¹ yr⁻¹ (fish meat), and 4180 kg C ha⁻¹ yr⁻¹ (corn seed). The total C input was 6400 kg C ha⁻¹ yr⁻¹, which is near the high end of the applications reported for fish ponds (from 1200 to 9900 kg C ha⁻¹ yr⁻¹; Zhao et al., 2021).

Our observation site was located in the enclosure aquaculture farm (31°03'40"N, 120°28'14"E; Fig. 1). The change in aquatic vegetation around the observation site caused by ecological restoration is shown in Fig. S1. Before ecological restoration, the enclosure aquaculture farm was dominated by submerged macrophytes, mainly *Elodea nuttallii*, *Hydrilla verticillate*, and *Vallisneria spiralis*. After ecological restoration, transparency reduction caused by sediment resuspension under wind disturbance inhibited the growth of submerged macrophytes, and floating-leaved plants, mainly *Trapa natans*, became the dominant species.

2.2. Eddy covariance and microclimate measurements

We employed the EC method to measure the CO₂ and the CH₄ fluxes.

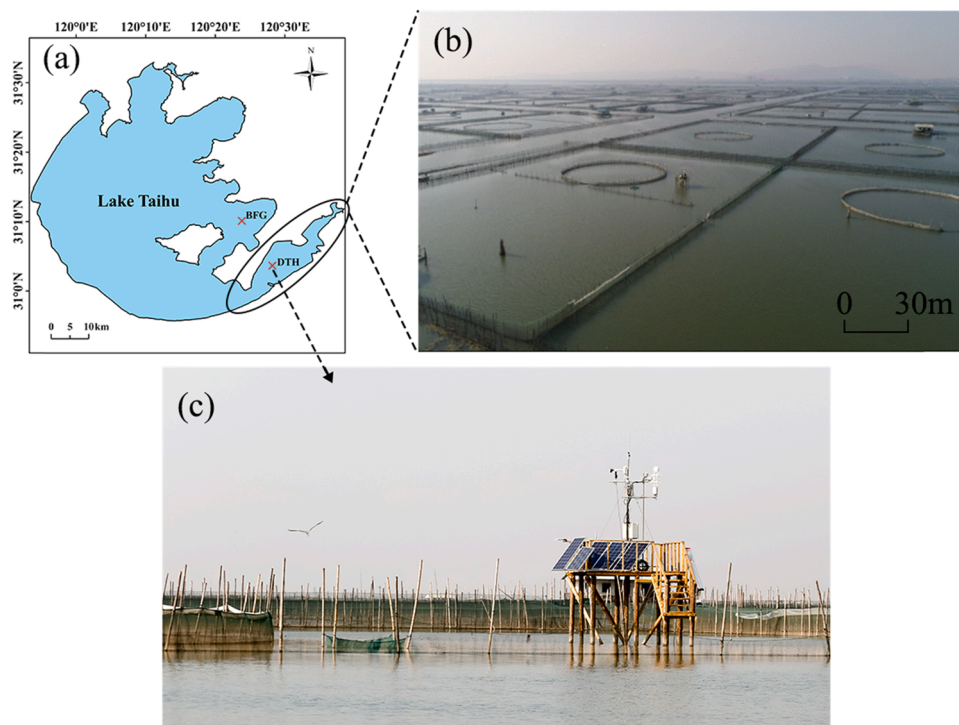


Fig. 1. Site location and photos: (a) Map of Lake Taihu showing the location of the observation site in this study (DTH) and the reference site (BFG); (b) Aerial photo of the aquaculture farm (date: November 2017); (c) Photo of the measurement platform and instrumentation.

The EC observational system consisted of a sonic anemometer/thermometer (Model CSAT3A, Campbell Scientific Inc., Logan, UT, USA), an open-path CO₂/H₂O analyzer (Model EC150, Campbell Scientific Inc.), and an open-path CH₄ analyzer (Model Li-7700, LI-COR Inc., Lincoln, NE, USA). The sampling frequency was 10 Hz, and the raw data was recorded by a data logger (Model CR3000, Campbell Scientific Inc.). The EC system was installed at a height of about 5 m above the water surface on a platform about 2 km away from the nearest shore (Fig. 1). The observation started in March 2018 and has continued to date. The results reported here covered the period from March 2018 to December 2020.

Micrometeorological variables were measured simultaneously with the EC observation, including air temperature and humidity (Model HMP155, Vaisala Inc., Helsinki, Finland), atmospheric pressure (Model CS106, Campbell Scientific Inc.), wind speed and wind direction (Model 05103, R M Young Company, Traverse City, Michigan, USA), four components of the radiation balance (Model CNR4, Kipp & Zonen B.V., Delft, the Netherlands), water temperature at the depths of 20 and 50 cm and sediment temperature at the depth of 3 cm below the water column (Model 109-L, Campbell Scientific Inc.). These meteorological variables were sampled at 1 Hz and averaged to half-hour intervals by a data logger (Model CR3000, Campbell Scientific Inc.). The water depth was extracted from monthly hydrological reports from Taihu Basin Authority of Ministry of Water Resources. Precipitation was measured at the Dongshan surface weather station maintained by the China Meteorological Data Network, which is about 5.6 km to the northwest of the platform.

2.3. Processing and gap-filling of eddy covariance data

The raw 10-Hz EC data was processed to produce 30-min fluxes using the EddyPro software (version 6.2.1, LI-COR, Lincoln). Before the flux calculation, the 10-Hz data was screened for spikes, de-trended with the block averaging method, and were compensated for time lags (Vickers and Mahrt, 1997; Horst and Lenschow, 2009). A double coordinate rotation was performed to align the streamwise velocity component to the horizontal wind and to force the mean vertical wind velocity to zero

for each 30-min observation (Kaimal and Finnigan, 1994; Baldocchi et al., 2000). The sensible heat flux was corrected for the effect of humidity fluctuations (Schotanus et al., 1983). The WPL density correction was applied to eliminate the effects of temperature and water vapor fluctuations on the water vapor, CO₂, and CH₄ fluxes (Webb et al., 1980). The spectroscopic correction was carried out to eliminate the effects of gas temperature, pressure and water vapor on the shape of the absorption line of CH₄ (Rothman et al., 2009). Corrections for flux loss at high frequencies were made with a standard cospectral model (Moore, 1986; Moncrieff et al., 1997).

The 30-min flux data were tagged with the 0–1–2 flag system (Mauder and Foken, 2004), corresponding to high-quality, intermediate-quality, and poor-quality. The flux data with flag 2 were discarded from further analysis. Additionally, the criteria of the signal strength were set to 10% and 0.85 for CH₄ and CO₂, respectively, and the data with the signal strength lower than these criteria were omitted. A total of 26549 half-hourly CH₄ observations remained after the above data screening procedure, representing 50% of the time between January 2018 and December 2020.

We did not fill half-hourly data gaps. If the valid 30-min CH₄ flux data in a day exceeded 40%, a daily average flux was calculated. The percent of valid daily CH₄ flux was 56%, 67%, and 58% in 2018, 2019, and 2020, respectively. The daily CH₄ flux gaps were filled with a random forest (RF) technique. Compared with other machine learning algorithms, RF has better performance in CH₄ flux gap-filling due to its stronger ability to deal with nonlinear problems and avoiding overfitting (Xu et al., 2018; Kim et al., 2020). We used eight ancillary environment variables as input features, including incoming shortwave radiation, sediment temperature, water depth, wind speed, atmospheric pressure, relative humidity, precipitation, and day of year. The number of leaf nodes was set to five to minimize the mean square error. All valid daily flux data in that year was separated into a training set (70%) and a test set (30%). The test set was used to validate the performance of the model. RF predictions for daily CH₄ flux gave a modeled R² of 0.92, 0.96, and 0.88 with a RMSE of 0.44, 0.21, and 0.28 μg CH₄ m⁻² s⁻¹ in 2018, 2019, and 2020, respectively, indicating that the RF gap-filling method

performed very well. The monthly mean flux and the annual flux were based on the gap-filled daily flux time series.

2.4. CH₄ ebullition flux

The eddy-covariance CH₄ ebullition flux partitioning was based on the method developed by Iwata et al. (2018). Using the local scalar similarity between the CH₄ concentration and another reference scalar, such as water vapor concentration or air temperature, in the wavelet time-scale domain, the method assumes that the dissimilar fluctuating components between them result from ebullition. In this study, the reference scalar was air temperature. A wavelet transform was performed on the CH₄ concentration and the reference scalar to obtain their respective wavelet coefficients. For each 30-min, a fitting regression line between the wavelet coefficients for CH₄ concentration and air temperature was determined by the iteratively-reweighted least-squares method. For each month, the minimum of root mean squared deviation (RMSD) from the regression line was interpreted as an appropriate bound in that month. Here we used $\pm 3 \times \text{RMSD}$ as the bounds and assumed that the coefficients outside the bounds corresponded to the CH₄ ebullition emission.

2.5. CH₄ diffusion flux

The transfer coefficient method was used to measure the CH₄ diffusion flux during the restoration period. The measurement was carried out once every one to two months during site visits. In total, there were 12 and 5 observations in 2019 and 2020, respectively. In each observation, two 30-mL water samples were collected at the depth of 20 cm at a distance of about 2 m from the EC platform using 60-mL gas-tight syringes. Next, a volume of 30-mL pure N₂ was injected into the syringe, which was shaken vigorously for 3 min and then left for 5 min to reach the gas-liquid equilibrium. The gas sample was injected into a 50-mL vacuum bag made of aluminum foil and brought back to the laboratory. Determination of the CH₄ concentration was made with a gas chromatograph (Model GC7890B, Agilent Technologies Inc., Santa Clara, CA, USA) within 24 h of sampling. The dissolved CH₄ concentration in water was calculated using Dalton's law of partial pressure and Henry's law.

The CH₄ diffusion flux at the water-air interface was calculated as follows:

$$F_m = k \times (C_w - C_{eq})$$

where k is the gas exchange coefficient, C_w is the dissolved CH₄ concentration at the depth of 20-cm from the water surface, and C_{eq} is the CH₄ concentration in water in equilibrium with the atmosphere under in-situ conditions. Atmospheric CH₄ concentration was measured by Li-7700. In this study, the k value was estimated using four models proposed by Cole and Caraco (1998), Vachon and Prairie (2013), Read et al. (2012), and Heiskanen et al. (2014).

The CH₄ diffusion contribution was the ratio of the diffusion flux measured by the transfer coefficient method to the total flux measured by the EC method. To match these two measurements in the time, we used the mean EC flux over two hours centered at the time of water sampling.

2.6. Classification of aquatic vegetation types

To explore the potential effects of aquatic plant succession on the CH₄ flux and its emission pathways, aquatic vegetation types were classified once a month using Sentinel-2 satellite images with a spatial resolution of 10 m. We used the emergent vegetation sensitivity index for emergent plants, the normalized difference vegetation index for floating-leaved vegetation, and the submerged vegetation sensitivity index for submerged vegetation. The band combinations for these

indices are described by Luo et al. (2014). A classification decision tree was constructed to assign pixels in the order of emergent plants, floating-leaved vegetation, submerged vegetation, and open water. The segmentation thresholds are provided by Yang et al. (2021) who showed that the overall accuracy of this classification method is 83% for Lake Taihu.

2.7. Data analysis

Linear regression was used to examine the relationships (1) between the CH₄ diffusion flux measured by the transfer coefficient method and the total flux measured by the EC method; (2) between half-hourly CH₄ flux and net ecosystem productivity (NEP); (3) between monthly CH₄ flux and the percentage of vegetation coverage. Exponential regression was performed to investigate the effect of sediment temperature on daily and monthly CH₄ flux.

3. Results

3.1. General environmental conditions

The air temperature, water temperature, and sediment temperature in East Lake Taihu exhibited similar and obvious seasonal patterns during the three years, with the highest temperatures in August and the lowest in January (Fig. 2a). The ranges of monthly mean air temperature were 4.0–29.6 °C, 5.7–28.9 °C, and 6.6–30.5 °C in 2018, 2019, and 2020, respectively, and the corresponding ranges of monthly mean sediment temperature were 6.3–29.5 °C, 6.7–28.6 °C, and 7.3–27.2 °C. Wind speed did not show clear seasonal variations but usually peaked in July or August due to frequent storms, especially in 2018 and 2019. The annual mean wind speed was 3.6 m s⁻¹ in 2019 and 3.9 m s⁻¹ in 2020, both of which were higher than the mean wind speed of 3.2 m s⁻¹ in 2018 (Fig. 2b). The increase in wind speed was caused by seine net removal, not by changes in the local background climate because wind speed at BFG, a lake site outside the aquaculture zone (Fig. 1a), did not show appreciable inter-annual variability (mean wind speed 4.8, 4.3, and 4.6 m s⁻¹ in 2018, 2019 and 2020, respectively). The incoming solar radiation was generally higher in the summer months (June to August) than in other months except for June (cumulative precipitation: 254 mm) and July (cumulative precipitation: 356 mm) 2020 due to excessive rainy weather (Fig. 2c). The water depth was greater than 1 m, with the maximum in July to September (Fig. 2c). Water depth in July 2020 was exceptionally high, reaching a value of 2.5 m.

During the summer of 2018, the last year of aquaculture, the percentage of submerged plant coverage was much higher than that of floating-leaved plant coverage (Fig. S2 top panels). There was an in-phase relationship between the two vegetation types, with both peaking in the summer (Fig. 4a). The area of floating-leaved vegetation increased rapidly in 2019 and 2020, almost extending the whole footprint in the summer of 2020 (Fig. S2 bottom panels; Fig. S1 panel c). On average, the percentage of floating-leaved plant coverage was 25%, 64%, and 79% within the footprint in the peak growing season (June to October) in 2018, 2019, and 2020, respectively, and the corresponding submerged plant coverage was 60%, 29%, and 15%.

3.2. Temporal variations of CH₄ flux at different time scales

Over the annual period, the highest CH₄ emission was observed between DOY (day of year) 200 and DOY 260 (Fig. 3a). In general, the CH₄ flux was lower after ecological restoration than that before ecological restoration, with the maximum daily mean flux of 6.60, 4.88, and 4.36 μg CH₄ m⁻² s⁻¹ in 2018, 2019, and 2020, respectively. About 8.4%, 2.5%, and 1.1% half-hourly observations exceeded 5 μg CH₄ m⁻² s⁻¹ in 2018, 2019, and 2020, respectively (Fig. 3b).

The CH₄ flux diurnal pattern was different between the growing season and the non-growing season and between years (Fig. S3;

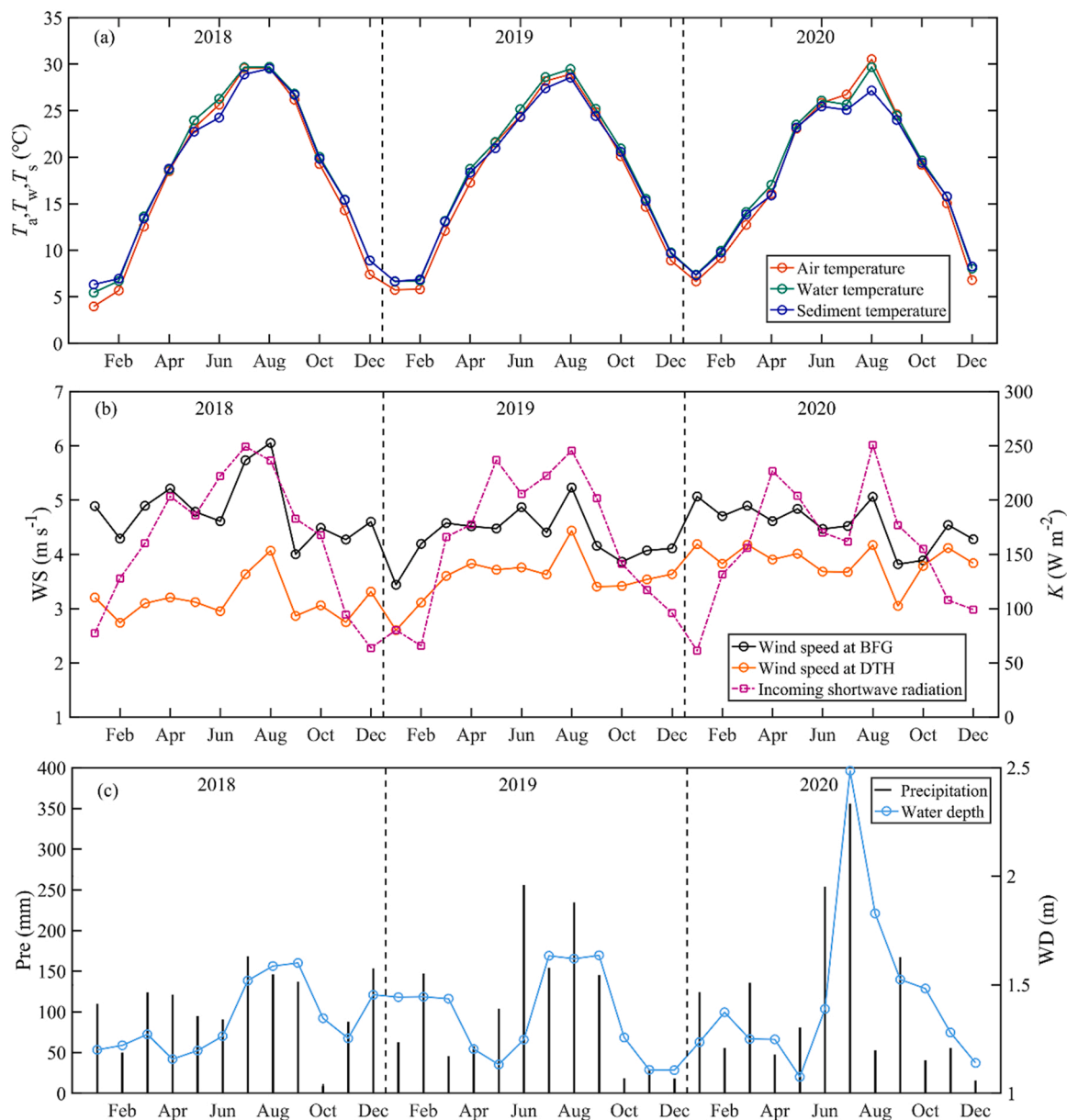


Fig. 2. Monthly mean meteorological variables and water depth in East Lake Taihu: (a) air temperature (T_a), water temperature (T_w), and sediment temperature (T_s); (b) wind speed (WS) and incoming shortwave radiation (K); (c) precipitation (Pre) and water depth (WD).

Table S1). The diurnal variation was rather weak in 2018, with the nighttime (20:00–04:00 local time) flux about 10% and 20% higher than the daytime (08:00–16:00 local time) flux during the growing and non-growing season, respectively (**Table S1**). During 2019 (the first year of ecological restoration), the CH_4 flux showed a conspicuous unimodal pattern, with the nighttime flux 41% and 64% higher than the daytime flux during the growing and non-growing season. The CH_4 flux during the 2020 growing season changed to a bimodal W-shaped pattern, with peak values around noon and at midnight, with a higher mean daytime flux than nighttime flux.

The CH_4 flux showed similar seasonal variations among the three years but with different emission levels (**Fig. 4b**). In the cold season (November to April), there was little difference in the monthly mean CH_4 flux during the three years. The warm-season flux showed large inter-annual variabilities, with the highest value in 2018 and the lowest value in 2020. If only July, August, and September were considered, the average CH_4 flux was 3.90, 2.52, and 2.01 $\mu\text{g CH}_4 \text{ m}^{-2} \text{ s}^{-1}$ in 2018, 2019, and 2020, respectively. The annual mean CH_4 flux was 1.52, 1.00,

and 0.96 $\mu\text{g CH}_4 \text{ m}^{-2} \text{ s}^{-1}$, in 2018, 2019, and 2020, respectively.

The cumulative C- CH_4 emission was much higher before ecological restoration than after restoration. The difference in the cumulative emission in the three years was not obvious before DOY 150. Afterwards, the cumulative emission increased much more slowly as season progressed in 2019 and 2020 than in 2018. The annual cumulative C- CH_4 emission was 36.0, 23.7, and 22.8 g C m^{-2} in 2018, 2019, and 2020, respectively (**Fig. S4**).

3.3. The roles of ebullition and diffusion

Ebullition was the dominant pathway of the CH_4 flux. The monthly median ebullition ratio was in the range of 40–67%, 42–78%, and 50–76% in 2018, 2019, and 2020, respectively (**Fig. S5**). The growing season ebullition ratio was slightly lower in 2018 (median value 59%) than in 2019 (median value 67%) and 2020 (median value 61%; **Fig. 5**).

The mean values of k calculated with four different models were 1.20, 2.86, 1.81, and 2.15 m d^{-1} , respectively (**Table S2**), corresponding

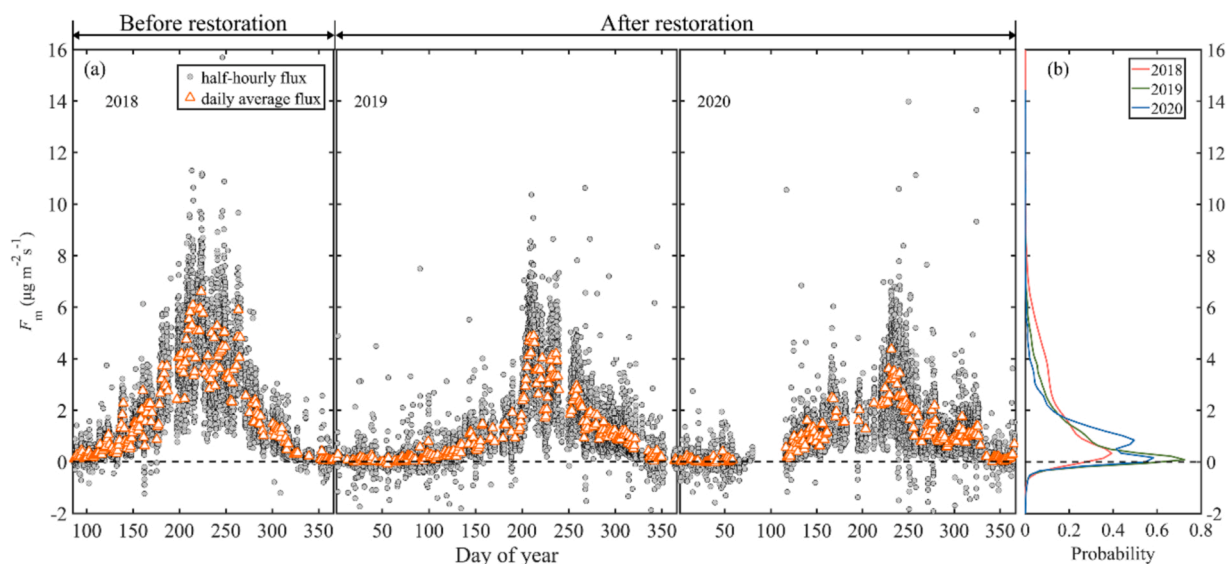


Fig. 3. (a) Time series of CH₄ flux. Gray solid circles and orange open triangles denote half-hourly and daily mean CH₄ flux, respectively; (b) Probability distribution of half-hourly CH₄ flux.

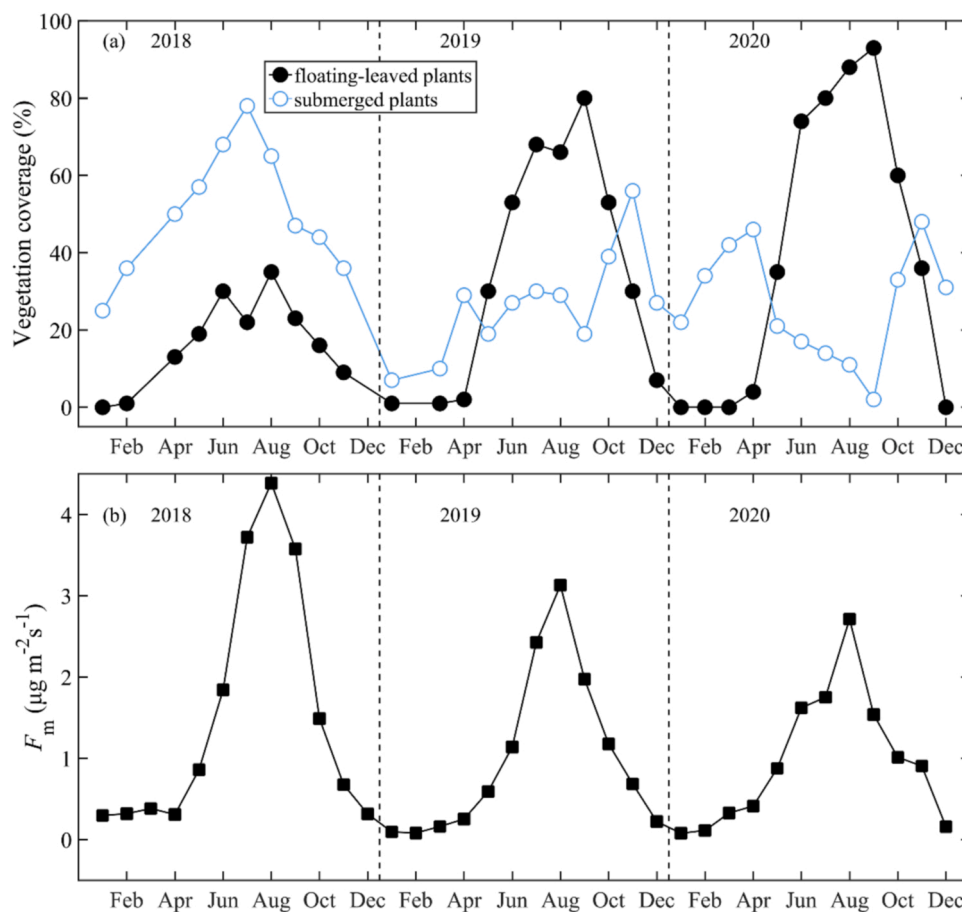


Fig. 4. (a) Time series of percentage of floating-leaved and submerged plant coverage within the EC flux footprint. Black solid circles and blue open circles denote percentage of floating-leaved plant coverage and submerged plant coverage, respectively; (b) Time series of monthly mean CH₄ flux.

to mean CH₄ diffusion flux of 0.10, 0.23, 0.13 and 0.17 $\mu\text{g CH}_4 \text{ m}^{-2} \text{ s}^{-1}$. The diffusion flux was less important than the ebullition flux. Based on the four models, the slope of the fitted line between the diffusion flux and the corresponding total flux was 0.13, 0.30, 0.15, and 0.22 (Fig. 6), respectively, implying a contribution of about 13–30%. The mean

diffusion flux in the summer, based on a total of 6 diffusion flux measurements from June to August, was 0.13–0.33 $\mu\text{g CH}_4 \text{ m}^{-2} \text{ s}^{-1}$. The mean eddy flux during these summer sampling times was 1.17 $\mu\text{g CH}_4 \text{ m}^{-2} \text{ s}^{-1}$, yielding a diffusion flux contribution of 11–28%.

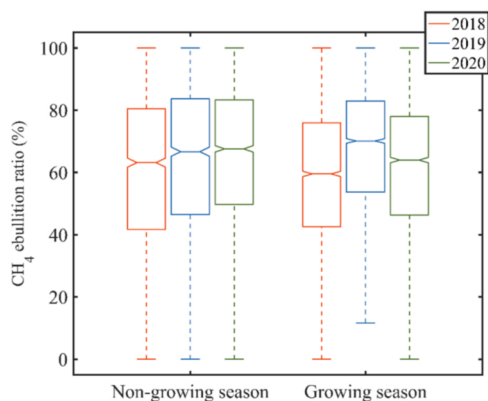


Fig. 5. Boxplot of half-hourly CH_4 ebullition ratio in the non-growing season and the growing season. The notch, the bottom, and the top edge of each boxplot represent the median value, the 25th, and 75th percentile, respectively. The whiskers indicate $\pm 1.5 \times$ interquartile ranges.

3.4. Factors controlling the CH_4 flux

The daily CH_4 flux showed an exponential dependence on sediment temperature, with the exponential fit explaining more than 83% of the observed variations in the CH_4 flux (Fig. 7; Table S3). At the same temperature, the CH_4 flux was lower in the warming phase (from the first day to the day with maximum daily sediment temperature) than the cooling phase (from the day with maximum daily sediment temperature to the last day) of the year. This hysteresis response to temperature was

especially obvious in the temperature range of 15–25 °C. The exponential function described the temperature-dependent relationship better if the two phases were treated separately (Table S3). The temperature sensitivity during the warming phase gradually increased with the restoration time, with the Q_{10} value increasing from 8.17 in 2018 to 9.30 in 2019 and 10.38 in 2020. In comparison, the temperature sensitivity during the cooling phase was relatively stable, with the Q_{10} value of 3.25, 3.53, and 2.94 for 2018, 2019, and 2020, respectively. Similar relationships were observed for the monthly flux (Fig. 8; Table S4).

The daytime (08:00–16:00 local time) CH_4 flux showed a poor correlation with the NEP in 2018 (Fig. 9a; $p = 0.32$). This correlation became positive and highly significant in 2019 and 2020 (Fig. 9b & c; $p < 0.001$). The slope of the fitting regression line was greater in 2020 than that in 2019, indicating that the daytime CH_4 flux responded more strongly to the changes of NEP in 2020 than in 2019.

Vegetation coverage was another factor controlling the CH_4 flux on the monthly scale. Although the monthly CH_4 flux increased with the increasing vegetation coverage in each of the three years, the positive correlation passed the significance test only after ecological restoration ($p = 0.08$ in 2018; $p < 0.01$ in 2019; $p < 0.001$ in 2020; Fig. S6).

4. Discussion

4.1. Effects of aquaculture and ecological restoration on lake CH_4 flux

During the aquaculture period, the gap-filled annual CH_4 flux of East Lake Taihu was $1.52 \mu\text{g CH}_4 \text{ m}^{-2} \text{ s}^{-1}$ or $36.0 \text{ g C m}^{-2} \text{ yr}^{-1}$. This value was one order of magnitude higher than the annual flux of 6.12 g C m^{-2}

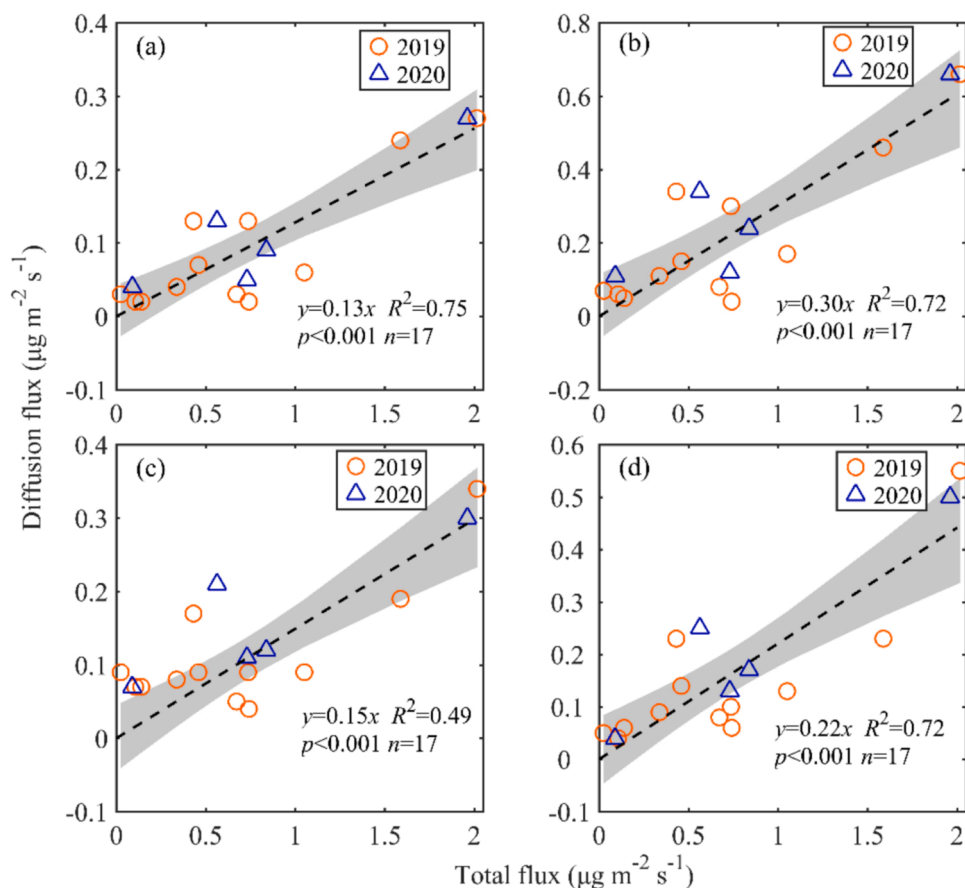


Fig. 6. Comparison of the diffusion CH_4 flux calculated with four different models of the gas transfer coefficient and the total flux measured with the EC method: (a) Cole and Caraco (1998) model; (b) Vachon and Prairie (2013) model; (c) Read et al. (2012) model; (d) Heiskanen et al. (2014) model. The black dotted line represents the best fit regression with statistics noted, and the gray shadow represents the 95% confidence bound.

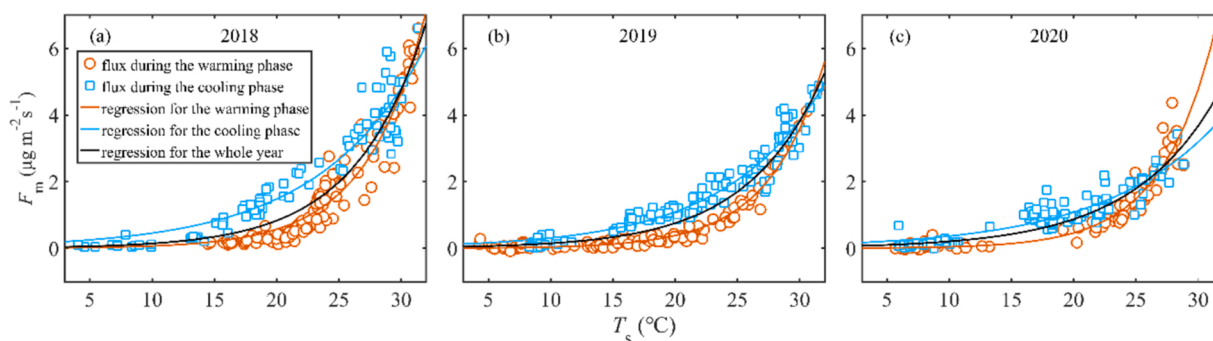


Fig. 7. Relationships between daily mean CH_4 flux (F_m) and sediment temperature (T_s). The regression statistics are given in Table S3.

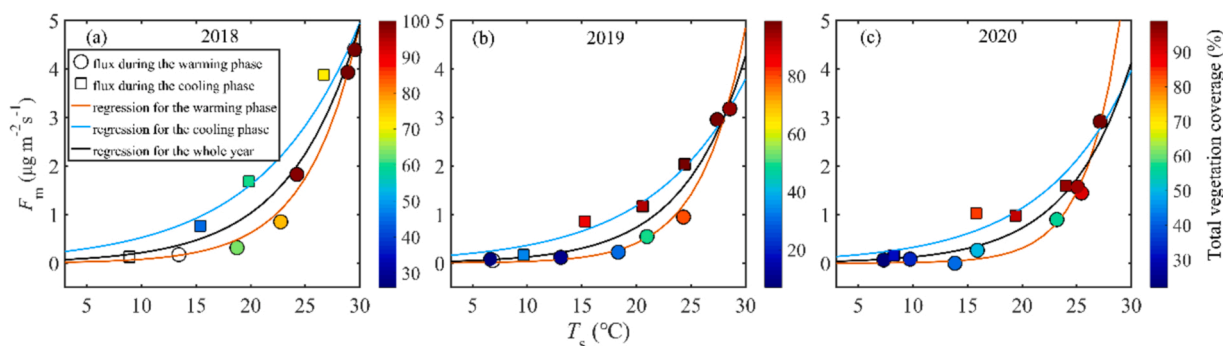


Fig. 8. Relationships between monthly mean CH_4 flux (F_m) and sediment temperature (T_s). Color indicates total vegetation coverage. The regression statistics are given in Table S4.

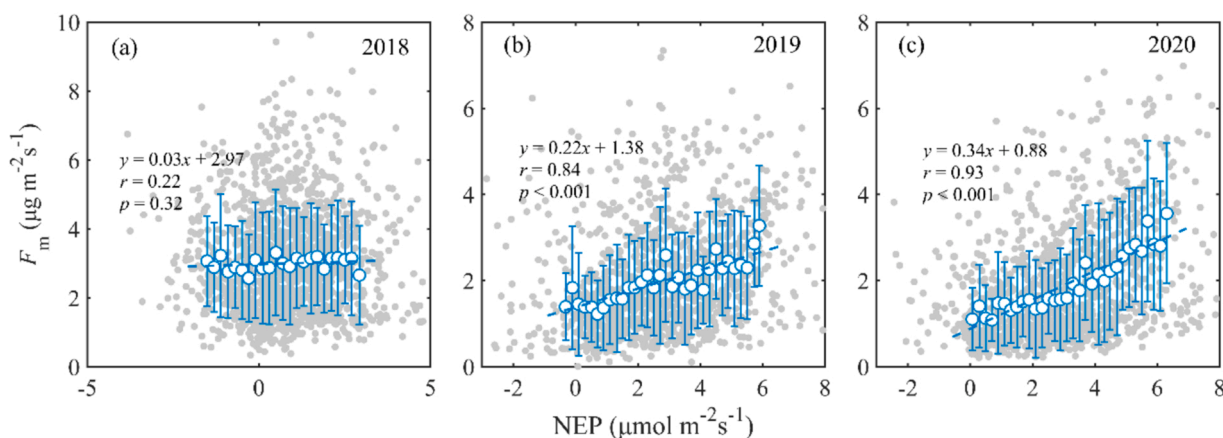


Fig. 9. Relationships between the CH_4 flux and NEP at the half-hourly scale between 08:00 and 16:00 local time in the growing season. Gray dots represent half-hourly data, and blue open circles represent the bin-averaged data. Error bars are \pm one standard deviation of average half-hourly values.

yr^{-1} reported for a zone with submerged vegetation (BFG, Fig. 1a; Zhang et al., 2019) and $1.35 \text{ g C m}^{-2} \text{ yr}^{-1}$ for an open-water eutrophic zone of Lake Taihu (Xiao et al., 2014). These differences indicate that aquaculture activities exerted an enormous influence on the lake CH_4 emission. The total amount of feed was $6400 \text{ kg C ha}^{-1}$ in 2018. These feed materials had abundant protein and starch which are easier to be decomposed into methanogenic substrates than plant residues (Xu et al., 2020).

The mean CH_4 emission in 2019 and 2020 was $0.98 \mu\text{g CH}_4 \text{ m}^{-2} \text{ s}^{-1}$ or $23.2 \text{ g C m}^{-2} \text{ yr}^{-1}$, representing a decrease of 36% from the pre-ecological restoration value. This trend is consistent with the global synthesis study by Rosentreter et al. (2021) showing a CH_4 emission decrease along the gradient of impacted to natural aquatic ecosystems. In a regional synthesis study by Kumar et al. (2019) on CH_4 emission in

lakes in China, the annual CH_4 emission ranges from 0.002 to $0.90 \mu\text{g CH}_4 \text{ m}^{-2} \text{ s}^{-1}$ with a mean of $0.19 \mu\text{g CH}_4 \text{ m}^{-2} \text{ s}^{-1}$. The lakes analyzed by Kumar et al. (2019) were not impacted by aquaculture activities, so the large contrast between their low emission values and the flux observed in year 1 and year 2 after the abandonment of aquaculture suggests a long recovery time for East Lake Taihu to reach a new natural state. According to Jones and Schmitz (2009), the time for an ecosystem to recover from disturbance depends on the severity of disturbance. They found that it takes 10–20 years for freshwater ecosystems that have experienced eutrophication, species invasion, or overfishing to recover to an undisturbed state. It is interesting that in the present study, the rate of flux decrease was 34% from 2018 to 2019 but was only 4% from 2019 to 2020. The slower decline in 2020 may be attributed to the significant increase in aquatic vegetation (Fig. S2 bottom panels; Fig. 4a), which

provides substrate for CH₄ production (Ström et al., 2007; Laanbroek et al., 2010), thus offsetting the impact of removal of aquafeed input. This confounding effect associated with vegetation growth may force the lake zone to recover to a steady state different from pre-disturbed conditions.

4.2. Comparison with other aquaculture systems

In a meta analysis of aquaculture CH₄ emission data, Yuan et al. (2019) showed that the mean annual CH₄ flux is 64.2 g C m⁻² yr⁻¹ (2.71 μg m⁻² s⁻¹) from extensive aquaculture (low stocking density and no aerator facilities) and 34.7 g C m⁻² yr⁻¹ (1.47 μg m⁻² s⁻¹) from semi-intensive systems (higher stocking density and intermittent aeration). They found that the emission from intensive aquaculture, defined as systems which have high stocking rates and continuous aeration or frequent water exchange, is negligible. This result is based on measurements in fish tanks and aquaponics which lack habitats for methanogens. They suggest that enclosure aquaculture belongs to the intensive category because of the high stocking rate and sufficient dissolved oxygen from the constant exchange of water in the enclosure with the surrounding. Our observed annual emission (36.0 g C m⁻² yr⁻¹) was in close agreement with the mean flux of semi-intensive systems, implying that the semi-intensive category may be a more appropriate characterization for enclosure aquaculture. Based on the data collected with floating chambers in six sampling days throughout the year, da Silva et al. (2018) reported a high mean flux of 6.5 μg CH₄ m⁻² s⁻¹ for net cage aquaculture in a hydropower reservoir in Brazil.

In a recent survey of the aquaculture literature, Zhao et al. (2021) showed that dredging may exert a much larger influence on the CH₄ emission flux than aeration. They reported that the mean annual flux is 2.32 μg m⁻² s⁻¹ (54.8 g C m⁻² yr⁻¹) for pond systems without dredging and only 0.17 μg m⁻² s⁻¹ (4.0 g C m⁻² yr⁻¹) for ponds with dredging. Pond systems without dredging have much higher fluxes because of long-term accumulation of organic substrate in the sediment. That our research site has never been dredged may have been a reason for why the site behaved like a semi-intensive system and for why the flux remained high in 2019 and 2020 despite of no input of feed materials.

Our result suggests that the CH₄ emission from intensive aquaculture systems may have been underestimated by Yuan et al. (2019). The middle and lower reaches of Yangtze River are the main regions of lake aquaculture, accounting for 50% of the total lake aquaculture in China (China Fishery Statistical Yearbook, 2019). Given that the aquaculture lakes in this area experience similar climates and are characterized by shallow water depth, we assume that the annual mean CH₄ flux observed in East Lake Taihu in 2018 represents the CH₄ emission level of these lakes and estimate that CH₄ emission from enclosure aquaculture in these areas was 130 Gg C yr⁻¹, which is about 3% of the total emission from global freshwater aquaculture systems (Yuan et al., 2019) and 9% of the total emission from natural lakes in China (Li et al., 2018).

4.3. The role of aquatic vegetation in lake CH₄ flux

Our results support the view that aquatic vegetation can influence the lake CH₄ emission via multiple pathways. Photosynthesis causes plant roots to produce soluble exudates. These root exudates contain small carbon molecules, e.g., amino acids, which are relatively easy to be decomposed into methanogenic substrates by microorganisms (Waldo et al., 2019). Availability of root exudates may be the reason for the significant positive correlation between the monthly CH₄ flux and vegetation coverage after ecological restoration (Fig. S6b & c). However, we did not observe a strong correlation for 2018 despite the presence of substantial submerged plants. This may be related to the large amount of allochthonous feed input, which masked the role of root exudates in promoting CH₄ production.

Floating-leaved plants can serve as a conduit transporting CH₄ to the atmosphere. At present, the majority of published studies on this subject

have focused on emergent plants in wetlands and in lake littoral zones (e.g., Wang et al., 2006; Ström et al., 2007; Hamilton et al., 2014; Hu et al., 2016; Andresen et al., 2017). A few studies have also concluded that rooted floating-leaved plants can transport CH₄ through aerenchyma tissues and stomata (Bolpagni et al., 2007; Jeffrey et al., 2019; Oliveira Junior et al., 2020). In a chamber-based study of water lily (*Nymphaea odorata* Ait.), Villa et al. (2020) found that CH₄ emission flux is positively correlated with CO₂ uptake via stomata. Interestingly, they reported that the conductance of floating-leaved plants is 1.7 times higher than that of emergent species found in the same mineral-soil wetland. Here, to test whether CH₄ flux is regulated by stomata of floating-leaved plants, we analyzed the ecosystem-scale relationship between the daytime CH₄ flux and NEP in the growing season. A significant positive correlation appeared only after the recovery of floating-leaved plants (Fig. 9b & c), which may provide ecosystem-scale evidence for plant stomatal regulation of CH₄ flux, that is, plant CH₄ transport, although root exudates may have also played a role. In 2020, the CH₄ flux peaked at noon during the growing season (Fig. S3e), which could also be interpreted as evidence of plant-mediated transport. The seasonal hysteresis of the CH₄ flux shown in Fig. 8 can also be viewed as evidence of plant transport. This is because the higher flux occurred in the second half of the growing season when vegetation coverage was also higher than in the first half of the growing season. In a related study, water chestnut (*Trapa natans* L.), the dominant species in East Lake Taihu in 2019 and 2020 (Fig. S1b & c), almost triples the CH₄ emission during the daytime through aerenchyma tissues, in comparison to the adjacent water surface free of water chestnut (Bolpagni et al., 2007).

A third effect of floating-leaved plants is related to ebullition. A laboratory experiment revealed a significant positive correlation between the coverage of free-floating plants and the fraction of ebullition intercepted by plants (Kosten et al., 2016). In other words, floating leaves may serve as a physical barrier preventing CH₄-containing bubbles from escaping the water column. Although some intercepted bubbles may be released by wind disturbance, others may stay on the plants for long enough time to allow oxidation of CH₄ trapped in them. In the present study, the method for determining the CH₄ ebullition ratio was too noisy for detection of an inter-annual trend (Fig. S5; Fig. 5). Furthermore, the barrier effect may have been masked by the change of bottom shear stress due to purse seine removal. A previous study demonstrated that the existence of purse seine in East Lake Taihu reduces the bottom shear stress by 10–40% (Zhu, 2012). Because shear stress at the sediment surface is a key mechanism that triggers CH₄ ebullition (Joyce and Jewell, 2003), reduction in ebullition due to floating leaves may have been offset by the increase of ebullition due to the increase of bottom shear stress.

A crude estimate of the net vegetation effect can be obtained with the data collected during the water-air exchange observations (Fig. 6). The diffusion flux accounted for 20% ± 8% (mean ± one standard deviation, *n* = 4 based on the four diffusion coefficient models) of the total flux. The ebullition ratio, estimated with the method of eddy-covariance ebullition partitioning was 55% ± 23% (mean ± one standard deviation, *n* = 17). The residual (25%) can be regarded as the net plant contribution to the total flux.

4.4. Temperature sensitivity of CH₄ flux

Our study confirmed the widely observed exponential relationship between CH₄ flux and temperature. This relationship was, however, asymmetric between the warming and cooling phase of the annual cycle, with a lower flux during the warming phase at a given temperature. Bao et al. (2021) reported a much stronger CH₄ emission in Arctic tundra during autumn-freeze than during spring-freeze, and they suggest that substrate provided by dead aquatic vegetation in the autumn freeze boosts the abundance and activity of methanogens and CH₄ production. Kariyapperuma et al. (2018) observed a phenomenon in a liquid dairy manure pond similar to ours, where the CH₄ emission is much lower in

the warming phase than in the cooling phase of the year. In their study, the substrate concentration is higher in the warming phase than the rest of the year, and they hypothesized that the hysteresis may be related to the ability of methanogens to utilize the available substrate. Recently, a global synthesized study on wetland CH₄ cycling reported that 77% of site-years exhibit higher CH₄ emission later in the frost-free season than in earlier parts of the frost-free season (Chang et al., 2021). Our study shows that the hysteresis phenomenon also occurs in lake systems.

In the present study, the Q₁₀ value in the warming phase increased steadily over the three-year period. It is believed that a higher Q₁₀ value tends to be associated with a higher amount of organic substrate in lake systems (DelSontro et al., 2016; Iwata et al., 2020). However, the Q₁₀ value in 2018 was the lowest of the three years despite a large amount of aquafeed input, suggesting that other factors, such as biomass and activity of methanogens (DelSontro et al., 2016), may also affect the Q₁₀ value. In a laboratory experiment, plant root exudates stimulate the activity of microorganisms by changing the chemical environment in the soil, thereby reducing CH₄ oxidation around the roots and augmenting microbial utilization of carbon (Waldo et al., 2019). In a tundra wetland, the recovery of vegetation productivity is accompanied by more root exudates (Ström et al., 2003). We suggest that with ecological restoration in East Lake Taihu, root exudates may have increased rapidly with increasing floating-leaved vegetation abundance, contributing to the steady increase in Q₁₀ over the experimental period.

5. Summary

The key results of this study are as follows:

- (1) On the annual time scale, the enclosure aquaculture farm in East Lake Taihu was a large source of CH₄, emitting at a rate of 36.0 g C-CH₄ m⁻² yr⁻¹. The annual emission in year 1 and year 2 of ecological restoration was 36% lower than the pre-ecological restoration value, but was still much higher than the annual flux of lake systems not impacted by aquaculture farming. Possible reasons for the high flux after aquaculture abandonment included high shear stress at the sediment surface, carbon accumulated in the sediment over decades of aquaculture farming, and plant transport of CH₄.
- (2) On the daily and monthly time scale, sediment temperature was the dominant factor controlling the CH₄ flux. The flux response to sediment temperature was asymmetric, showing a higher CH₄ emission at the same temperature in the cooling phase than in the warming phase of the year. The Q₁₀ value of the warming phase increased steadily over time (8.17 in 2018, 9.30 in 2019, and 10.38 in 2020), possibly due to increased root exudates with rapidly increasing floating-leaved vegetation in the EC flux footprint.
- (3) On the half-hourly time scale, the CH₄ flux was positively correlated with the NEP during the growing season ($p < 0.001$) in year 1 and year 2 of ecological restoration, indicating that plant stomata regulated CH₄ flux. No significant correlation with the NEP was found in the growing season under aquaculture farming.

Declaration of Competing Interest

The authors declare that they have no known competing financial interests or personal relationships that could have appeared to influence the work reported in this paper.

Acknowledgments

This research was supported by the National Key R&D Program of China (grant number 2020YFA0607501 to WX), the National Natural Science Foundation of China (grant numbers 41575147 to MZ, 41975143 and 42021004 to WX), Chinese Postdoctoral Science

Foundation (2021M701755 to JYZ), and Open Fund from the Key Laboratory of Meteorology and Ecological Environment of Hebei Province, China (Z201901H to WX and Z202101B to JYZ).

Appendix A. Supporting information

Supplementary data associated with this article can be found in the online version at doi:10.1016/j.agee.2022.107883.

References

- Andresen, C.G., Lara, M.J., Tweedie, C.E., Lougheed, V.L., 2017. Rising plant-mediated methane emissions from arctic wetlands. *Glob. Chang. Biol.* 23, 1128–1139. <https://doi.org/10.1111/gcb.13469>.
- Baldocchi, D., Finnigan, J., Wilson, K., Paw, U., K.T., Falge, E., 2000. On measuring net ecosystem carbon exchange over tall vegetation on complex terrain. *Bound. Meteor.* 96, 257–291. <https://doi.org/10.1023/A:1002497616547>.
- Bao, T., Xu, X.Y., Jia, G.S., Billesbach, D.P., Sullivan, R.C., 2021. Much stronger tundra methane emissions during autumn freeze than spring thaw. *Glob. Chang. Biol.* 27, 376–387. <https://doi.org/10.1111/gcb.15421>.
- Bastviken, D., Cole, J., Pace, M., Tranvik, L., 2004. Methane emissions from lakes: dependence of lake characteristics, two regional assessments, and a global estimate. *Glob. Biogeochem. Cycles* 18, 1–12. <https://doi.org/10.1029/2004GB002238>.
- Bolpagni, R., Pierobon, E., Longhi, D., Nizzoli, D., Bartoli, M., Tomaselli, M., Viaroli, P., 2007. Diurnal exchanges of CO₂ and CH₄ across the water-atmosphere interface in a water chestnut meadow (*Trapa natans* L.). *Aquat. Bot.* 87, 43–48. <https://doi.org/10.1016/j.aquabot.2007.02.002>.
- Bostock, J., McAndrew, B., Richards, R., Jauncey, K., Telfer, T., Lorenzen, K., Little, D., Ross, L., Handisyde, N., Gatward, I., Corner, R., 2010. Aquaculture: global status and trends. *Philos. Trans. R. Soc. B Biol. Sci.* 365, 2897–2912. <https://doi.org/10.1098/rstb.2010.0170>.
- Chang, K.Y., Riley, W.J., Knox, S.H., Jackson, R.B., McNicol, G., Poulter, B., Aurela, M., Baldocchi, D., Bansal, S., Bohrer, G., Campbell, D.I., Cescatti, A., Chu, H., Delwiche, K.B., Desai, A.R., Euskirchen, E., Friborg, T., Goeckede, M., Helbig, M., Hemes, K.S., Hirano, T., Iwata, H., Kang, M., Keenan, T., Krauss, K.W., Lohila, A., Mammarella, I., Mitra, B., Miyata, A., Nilsson, M.B., Noormets, A., Oechel, W.C., Papale, D., Peichl, M., Reba, M.L., Rinne, J., Runkle, B.R.K., Ryu, Y., Sachs, T., Schäfer, K.V.R., Schmid, H.P., Shurpali, N., Sonnentag, O., Tang, A.C.I., Torn, M.S., Trotta, C., Tuittila, E.S., Ueyama, M., Vargas, R., Vesala, T., Windham-Myers, L., Zhang, Z., Zona, D., 2021. Substantial hysteresis in emergent temperature sensitivity of global wetland CH₄ emissions. *Nat. Commun.* 12. <https://doi.org/10.1038/s41467-021-22452-1>.
- China Fishery Statistical Yearbook, 2015. China Agriculture Press, Beijing.
- China Fishery Statistical Yearbook, 2019. China Agriculture Press, Beijing.
- Cole, J.J., Caraco, N.F., 1998. Atmospheric exchange of carbon dioxide in a low-wind oligotrophic lake measured by the addition of SF₆. *Limnol. Oceanogr.* 43, 647–656. <https://doi.org/10.4319/lo.1998.43.4.0647>.
- Covw, I.G., Ogutu-Owhayo, R., 2019. Towards sustainable fisheries and aquaculture management in the African Great Lakes. *Fish. Manag. Ecol.* 26, 397–405. <https://doi.org/10.1111/fme.12391>.
- da Silva, M.G., Packer, A.P., Sampaio, F.G., Marani, L., Mariano, E.V.C., Pazianotto, R.A.A., Ferreira, W.J., Alvalá, P.C., 2018. Impact of intensive fish farming on methane emission in a tropical hydropower reservoir. *Clim. Change* 150, 195–210. <https://doi.org/10.1007/s10584-018-2281-4>.
- Dai, X.L., Qian, P.Q., Ye, L., Song, T., 2016. Changes in nitrogen and phosphorus concentrations in Lake Taihu, 1985–2015. *J. Lake Sci.* 28, 935–943. <https://doi.org/10.18307/2016.0502> (in Chinese).
- Dai, Y.H., Feng, L., Hou, X.J., Choi, C.Y., Liu, J.G., Cai, X.B., Shi, L., Shi, L., Zhang, Y.L., Gibson, L., 2019. Policy-driven changes in enclosure fisheries of large lakes in the Yangtze plain: evidence from satellite imagery. *Sci. Total Environ.* 688, 1286–1297. <https://doi.org/10.1016/j.scitotenv.2019.06.179>.
- De Silva, S.S., 2012. Aquaculture: a newly emergent food production sector-and perspectives of its impacts on biodiversity and conservation. *Biodivers. Conserv.* 21, 3187–3220. <https://doi.org/10.1007/s10531-012-0360-9>.
- DelSontro, T., Boutet, L., St-Pierre, A., del Giorgio, P.A., Prairie, Y.T., 2016. Methane ebullition and diffusion from northern ponds and lakes regulated by the interaction between temperature and system productivity. *Limnol. Oceanogr.* 61, S62–S77. <https://doi.org/10.1002/lno.10335>.
- Food and Agriculture Organization of the United Nations (FAO), 2020. The State of World Fisheries and Aquaculture 2020: sustainability in action, Rome, Italy. <https://doi.org/10.4060/ca9229en>.
- Grasset, C., Mendonça, R., Villamor Saucedo, G., Bastviken, D., Roland, F., Sobek, S., 2018. Large but variable methane production in anoxic freshwater sediment upon addition of allochthonous and autochthonous organic matter. *Limnol. Oceanogr.* 63, 1488–1501. <https://doi.org/10.1002/lno.10786>.
- Hamilton, S.K., Sippel, S.J., Chanton, J.P., Melack, J.M., 2014. Plant-mediated transport and isotopic composition of methane from shallow tropical wetlands. *Inl. Waters* 4, 369–376. <https://doi.org/10.5268/IW-4.4.734>.
- Heiskanen, J.J., Mammarella, I., Haapanala, S., Pumpanen, J., Vesala, T., Macintyre, S., Ojala, A., 2014. Effects of cooling and internal wave motions on gas transfer coefficients in a boreal lake. *Tellus, Ser. B Chem. Phys. Meteorol.* 66, 1–17. <https://doi.org/10.3402/tellusb.v66.22827>.

- Horst, T.W., Lenschow, D.H., 2009. Attenuation of scalar fluxes measured with spatially-displaced sensors. *Bound.-Layer. Meteor.* 130, 275–300. <https://doi.org/10.1007/s10546-008-9348-0>.
- Hu, Q.W., Cai, J.Y., Yao, B., Wu, Q., Wang, Y.Q., Xu, X.L., 2016. Plant-mediated methane and nitrous oxide fluxes from a carex meadow in Poyang Lake during drawdown periods. *Plant Soil* 400, 367–380. <https://doi.org/10.1007/s11104-015-2733-9>.
- Hu, Z.Q., Wu, S., Ji, C., Zou, J.W., Zhou, Q.S., Liu, S.W., 2016. A comparison of methane emissions following rice paddies conversion to crab-fish farming wetlands in southeast China. *Environ. Sci. Pollut. Res.* 23, 1505–1515. <https://doi.org/10.1007/s11356-015-5383-9>.
- Iwata, H., Hirata, R., Takahashi, Y., Miyabara, Y., Itoh, M., Iizuka, K., 2018. Partitioning Eddy-covariance methane fluxes from a shallow lake into diffusive and ebullitive fluxes. *Bound.-Layer. Meteor.* 169, 413–428. <https://doi.org/10.1007/s10546-018-0383-1>.
- Iwata, H., Nakazawa, K., Sato, H., Itoh, M., Miyabara, Y., Hirata, R., Takahashi, Y., Tokida, T., Endo, R., 2020. Temporal and spatial variations in methane emissions from the littoral zone of a shallow mid-latitude lake with steady methane bubble emission areas. *Agric. For. Meteorol.* 295, 108184 <https://doi.org/10.1016/j.agrformet.2020.108184>.
- Jeffrey, L.C., Maher, D.T., Johnston, S.G., Kelaher, B.P., Steven, A., Tait, D.R., 2019. Wetland methane emissions dominated by plant-mediated fluxes: contrasting emissions pathways and seasons within a shallow freshwater subtropical wetland. *Limnol. Oceanogr.* 64, 1895–1912. <https://doi.org/10.1002/lno.11158>.
- Jia, P.Q., Zhang, W.B., Liu, Q.G., 2013. Lake fisheries in China: challenges and opportunities. *Fish. Res.* 140, 66–72. <https://doi.org/10.1016/j.fishres.2012.12.007>.
- Jones, H.P., Schmitz, O.J., 2009. Rapid recovery of damaged ecosystems. *PLOS One* 4. <https://doi.org/10.1371/journal.pone.0005653>.
- Joyce, J., Jewell, P.W., 2003. Physical controls on methane ebullition from reservoirs and lakes. *Environ. Eng. Geosci.* 9, 167–178. <https://doi.org/10.2113/9.2.167>.
- Kaimal, J.C., Finnigan, J.J., 1994. *Atmospheric Boundary Layer Flows: Their Structures and Measurements*. Oxford University Press., Oxford, UK.
- Kariyapperuma, K.A., Johannesson, G., Maldaner, L., VanderZaag, A., Gordon, R., Wagner-Riddle, C., 2018. Year-round methane emissions from liquid dairy manure in a cold climate reveal hysteretic pattern. *Agric. For. Meteorol.* 258, 56–65. <https://doi.org/10.1016/j.agrformet.2017.12.185>.
- Kim, Y., Johnson, M.S., Knox, S.H., Black, T.A., Dalmagro, H.J., Kang, M., Kim, J., Baldochi, D., 2020. Gap-filling approaches for eddy covariance methane fluxes: a comparison of three machine learning algorithms and a traditional method with principal component analysis. *Glob. Chang. Biol.* 26, 1499–1518. <https://doi.org/10.1111/gcb.14845>.
- Kosten, S., Piñeiro, M., de Goede, E., de Klein, J., Lamers, L.P.M., Ettwig, K., 2016. Fate of methane in aquatic systems dominated by free-floating plants. *Water Res.* 104, 200–207. <https://doi.org/10.1016/j.watres.2016.07.054>.
- Kumar, A., Yang, T., Sharma, M.P., 2019. Greenhouse gas measurement from Chinese freshwater bodies: a review. *J. Clean. Prod.* 233, 368–378. <https://doi.org/10.1016/j.jclepro.2019.06.052>.
- Laanbroek, H.J., 2010. Methane emission from natural wetlands: interplay between emergent macrophytes and soil microbial processes. A mini-review. *Ann. Bot.* 105, 141–153. <https://doi.org/10.1093/aob/mcp201>.
- Lee, X.H., Liu, S.D., Xiao, W., Wang, W., Gao, Z.Q., Cao, C., Hu, C., Hu, Z.H., Shen, S.H., Wang, Y.W., Wen, X.F., Xiao, Q.T., Xu, J.P., Yang, J.B., Zhang, M., 2014. The Taihu Eddy flux network: an observational program on energy, water, and greenhouse gas fluxes of a large freshwater lake. *Bull. Am. Meteorol. Soc.* 95, 1583–1594. <https://doi.org/10.1175/BAMS-D-13-00136.1>.
- Li, S.Y., Bush, R.T., Santos, I.R., Zhang, Q.F., Song, K.S., Mao, R., Wen, Z.D., Lu, X.X., 2018. Large greenhouse gases emissions from China's lakes and reservoirs. *Water Res.* 147, 13–24. <https://doi.org/10.1016/j.watres.2018.09.053>.
- Luo, J.H., Ma, R.H., Duan, H.T., Hu, W.P., Zhu, J.G., Huang, W.J., Lin, C., 2014. A new method for modifying thresholds in the classification of tree models for mapping aquatic vegetation in Taihu lake with satellite images. *Remote Sens* 6, 7442–7462. <https://doi.org/10.3390/rs6087442>.
- Mauder, M., Foken, T., 2004. Documentation and Instruction Manual of the Eddy Covariance Software Package TK2. University of Bayreuth, Department of Micrometeorology, Arbeitsergebnisse Nr. 26, pp. 42.
- Moncrieff, J.B., Massheder, J.M., de Bruin, H., Elbers, J., Friborg, T., Heusinkveld, B., Kabat, P., Scott, S., Soegaard, H., Verhoef, A., 1997. A system to measure surface fluxes of momentum, sensible heat, water vapour and carbon dioxide. *J. Hydrol.* 188–189, 589–611. [https://doi.org/10.1016/S0022-1694\(96\)03194-0](https://doi.org/10.1016/S0022-1694(96)03194-0).
- Moore, C.J., 1986. Frequency response corrections for eddy correlation systems. *Bound.-Layer. Meteor.* 37, 17–35. <https://doi.org/10.1007/BF00122754>.
- Oliveira Junior, E.S., van Bergen, T.J.H.M., Nauta, J., Budiša, A., Aben, R.C.H., Weideveld, S.T.J., de Souza, C.A., Muniz, C.C., Roelofs, J., Lamers, L.P.M., Kosten, S., 2020. Water Hyacinth's effect on greenhouse gas fluxes: a field study in a wide variety of tropical water bodies. *Ecosystems* 24, 988–1004. <https://doi.org/10.1007/s10021-020-00564-x>.
- Qin, B.Q., Xu, P.Z., Wu, Q.L., Luo, L.C., Zhang, Y.L., 2007. Environmental issues of Lake Taihu, China. *Hydrobiologia* 581, 3–14. <https://doi.org/10.1007/s10750-006-0521-5>.
- Read, J.S., Hamilton, D.P., Desai, A.R., Rose, K.C., MacIntyre, S., Lenters, J.D., Smyth, R.L., Hanson, P.C., Cole, J.J., Staehr, P.A., Rusak, J.A., Pierson, D.C., Brookes, J.D., Laas, A., Wu, C.H., 2012. Lake-size dependency of wind shear and convection as controls on gas exchange. *Geophys. Res. Lett.* 39, 1–5. <https://doi.org/10.1029/2012GL051886>.
- Rodríguez-Gallego, L., Meerhoff, E., Poersch, L., Aubriot, L., Fagetti, C., Vitancurt, J., Conde, D., 2008. Establishing limits to aquaculture in a protected coastal lagoon: impact of *Farfantepenaeus paulensis* pens on water quality, sediment and benthic biota. *Aquaculture* 277, 30–38. <https://doi.org/10.1016/j.aquaculture.2007.12.003>.
- Rosentrek, J.A., Borges, A.V., Deemer, B.R., Holgerson, M.A., Liu, S., Song, C., Melack, J., Raymond, P.A., Duarte, C.M., Allen, G.H., Oelofeldt, D., Poulter, B., Battin, T.I., Eyre, B.D., 2021. Half of global methane emissions come from highly variable aquatic ecosystem sources. *Nat. Geosci.* 14, 225–230. <https://doi.org/10.1038/s41561-021-00715-2>.
- Rothman, L.S., Gordon, I.E., Barbe, A., Benner, D.C., Bernath, P.F., Birk, M., Boudon, V., Brown, L.R., Campargue, A., Champion, J.P., Chance, K., Coudert, L.H., Dana, V., Devi, V.M., Fally, S., Flaud, J.M., Gamache, R.R., Goldman, A., Jacquemart, D., Kleiner, I., Lacombe, N., Lafferty, W.J., Mandin, J.Y., Massie, S.T., Mikhailenko, S.N., Miller, C.E., Moazzen-Ahmadi, N., Naumenko, O.V., Nikitin, A.V., Orphal, J., Perevalov, V.I., Perrin, A., Predoi-Cross, A., Rinsland, C.P., Rotger, M., Šimečková, M., Smith, M.A.H., Sung, K., Tashkun, S.A., Tennyson, J., Toth, R.A., Vandaele, A.C., Vander Auwera, J., 2009. The HITRAN 2008 molecular spectroscopic database. *J. Quant. Spectrosc. Radiat. Transf.* 110, 533–572. <https://doi.org/10.1016/j.jqsrt.2009.02.013>.
- Rutegwa, M., Gebauer, R., Veselý, L., Regenda, J., Strunecký, O., Hejzlar, J., Drozd, B., 2019. Diffusive methane emissions from temperate semi-intensive carp ponds. *Aquac. Environ. Interact.* 11, 19–30. <https://doi.org/10.3354/aei00296>.
- Schotanus, P., Nieuwstadt, F.T.M., De Bruin, H.A.R., 1983. Temperature measurement with a sonic anemometer and its application to heat and moisture fluxes. *Bound.-Layer. Meteor.* 26, 81–93. <https://doi.org/10.1007/BF00164332>.
- Shaher, S., Chanda, A., Das, S., Das, I., Giri, S., Samanta, S., Hazra, S., Mukherjee, A.D., 2020. Summer methane emissions from sewage water-fed tropical shallow aquaculture ponds characterized by different water depths. *Environ. Sci. Pollut. Res.* 27, 18182–18195. <https://doi.org/10.1007/s11356-020-08296-0>.
- Ström, L., Ekberg, A., Mastepanov, M., Christensen, T.R., 2003. The effect of vascular plants on carbon turnover and methane emissions from a tundra wetland. *Glob. Chang. Biol.* 9, 1185–1192. <https://doi.org/10.1046/j.1365-2486.2003.00655.x>.
- Ström, L., Lamppa, A., Christensen, T.R., 2007. Greenhouse gas emissions from a constructed wetland in southern Sweden. *Wetl. Ecol. Manag.* 15, 43–50. <https://doi.org/10.1007/s11273-006-9010-x>.
- Taoka, T., Iwata, H., Hirata, R., Takahashi, Y., Miyabara, Y., Itoh, M., 2020. Environmental controls on diffusive and ebullitive methane emissions at a sub-daily time scale in the littoral zone of a mid-latitude shallow lake. *J. Geophys. Res. Biogeosci.* 125 <https://doi.org/10.1029/2020JG005753>.
- Vachon, D., Prairie, Y.T., 2013. The ecosystem size and shape dependence of gas transfer velocity versus wind speed relationships in lakes. *Can. J. Fish. Aquat. Sci.* 70, 1757–1764. <https://doi.org/10.1139/cjfas-2013-0241>.
- Veenstra, J., Nolen, S., Carroll, J., Ruiz, C., 2003. Impact of net pen aquaculture on lake water quality. *Water Sci. Technol.* 47, 293–300. <https://doi.org/10.2166/wst.2003.0659>.
- Vickers, D., Mahrt, L., 1997. Quality control and flux sampling problems for tower and aircraft data. *J. Atmos. Ocean. Technol.* 14, 512–526. [https://doi.org/10.1175/1520-0426\(1997\)014<0512:QCAFSF>2.0.CO;2](https://doi.org/10.1175/1520-0426(1997)014<0512:QCAFSF>2.0.CO;2).
- Villa, J.A., Ju, Y., Stephen, T., Rey-Sanchez, C., Wrighton, K.C., Bohrer, G., 2020. Plant-mediated methane transport in emergent and floating-leaved species of a temperate freshwater mineral-soil wetland. *Limnol. Oceanogr.* 65, 1635–1650. <https://doi.org/10.1002/lno.11467>.
- Waldo, N.B., Hunt, B.K., Fadely, E.C., Moran, J.J., Neumann, R.B., 2019. Plant root exudates increase methane emissions through direct and indirect pathways. *Biogeochemistry* 145, 213–234. <https://doi.org/10.1007/s10533-019-00600-6>.
- Wang, H.J., Lu, J.W., Wang, W.D., Yang, L.Y., Yin, C.Q., 2006. Methane fluxes from the littoral zone of hypereutrophic Taihu Lake, China. *J. Geophys. Res. Atmos.* 111 <https://doi.org/10.1029/2005JD006864>.
- Wang, Q.D., Cheng, L., Liu, J.S., Li, Z.J., Xie, S.Q., De Silva, S.S., 2015. Freshwater aquaculture in PR China: trends and prospects. *Rev. Aquac.* 7, 283–302. <https://doi.org/10.1111/raq.12086>.
- Wang, R., Zhang, Y.X., Xia, W.T., Qu, X., Xin, W., Guo, C.B., Bowker, J., Chen, Y.S., 2018. Effects of aquaculture on lakes in the central Yangtze River Basin, China. I. water quality. *N. Am. J. Aquac.* 80, 322–333. <https://doi.org/10.1002/naaq.10038>.
- Wang, Y.T., Wang, W.C., Zhou, Z.Z., Xia, W., Zhang, Y.X., 2021. Effect of fast restoration of aquatic vegetation on phytoplankton community after removal of purse seine culture in Huayanghe Lakes. *Sci. Total Environ.* 768 <https://doi.org/10.1016/j.scitotenv.2020.144024>.
- Webb, E.K., Pearman, G.I., Leuning, R., 1980. Correction of flux measurements for density effects due to heat and water vapour transfer. *Q. J. R. Meteorol. Soc.* 106, 85–100. <https://doi.org/10.1002/qj.49710644707>.
- Wu, Q.L., 2001. On the sustainable development of fishery in East Taihu Lake. *J. Lake Sci.* 13, 337–344. <https://doi.org/10.18307/20010408> (in Chinese).
- Xia, Z.J., Jiang, Z.G., Xie, H., Guo, W.Y., Wang, C., 2018. Functional groups of fish community in the Huayang lake group and their response to enclosure culture. *Chin. J. Ecol.* 37, 438–445. <https://doi.org/10.13292/j.1000-4890.201802.006> (in Chinese).
- Xiao, C., Dou, W.F., Liu, G.H., 2010. Variation in vegetation and seed banks of freshwater lakes with contrasting intensity of aquaculture along the Yangtze River, China. *Aquat. Bot.* 92, 195–199. <https://doi.org/10.1016/j.aquabot.2009.11.007>.
- Xiao, W., Liu, S.D., Li, H.C., Xiao, Q.T., Wang, W., Hu, Z.H., Hu, C., Gao, Y.Q., Shen, J., Zhao, X.Y., Zhang, M., Lee, X.H., 2014. A flux-gradient system for simultaneous measurement of the CH₄, CO₂, and H₂O fluxes at a lake-air interface. *Environ. Sci. Technol.* 48, 14490–14498. <https://doi.org/10.1021/es5033713>.
- Xu, H.L., Li, H., Tang, Z.Z., Liu, Y., Li, G., He, Q., 2020. Underestimated methane production triggered by phytoplankton succession in river-reservoir systems: evidence from a microcosm study. *Water Res.* 185 <https://doi.org/10.1016/j.watres.2020.116233>.

- Xu, T., Guo, Z., Liu, S., He, X., Meng, Y., Xu, Z., Xia, Y., Xiao, J., Zhang, Y., Ma, Y., Song, L., 2018. Evaluating different machine learning methods for upscaling evapotranspiration from flux towers to the regional scale. *J. Geophys. Res. Atmos.* 123, 8674–8690. <https://doi.org/10.1029/2018JD028447>.
- Yang, J.Z.C., Luo, J.H., Lu, L.R., Sun, Z., Cao, Z.G., Zeng, Q.F., Mao, Z.G., 2021. Changes in aquatic vegetation communities based on satellite images before and after pen aquaculture removal in East Lake Taihu. *J. Lake Sci.* 33, 507–517. <https://doi.org/10.18307/2021.0228> (in Chinese).
- Yang, P., Zhang, Y.F., Lai, D.Y.F., Tan, L.S., Jin, B.S., Tong, C., 2018. Fluxes of carbon dioxide and methane across the water–atmosphere interface of aquaculture shrimp ponds in two subtropical estuaries: the effect of temperature, substrate, salinity and nitrate. *Sci. Total Environ.* 635, 1025–1035. <https://doi.org/10.1016/j.scitotenv.2018.04.102>.
- Yuan, J.J., Xiang, J., Liu, D.Y., Kang, H., He, T.H., Kim, S., Lin, Y.X., Freeman, C., Ding, W.X., 2019. Rapid growth in greenhouse gas emissions from the adoption of industrial-scale aquaculture. *Nat. Clim. Chang.* 9, 318–322. <https://doi.org/10.1038/s41558-019-0425-9>.
- Zeng, Q.F., Gu, X.H., Chen, X., Mao, Z.G., 2013. The impact of Chinese mitten crab culture on water quality, sediment and the pelagic and macrobenthic community in the reclamation area of Guchenghu Lake. *Fish. Sci.* 79, 689–697. <https://doi.org/10.1007/s12562-013-0638-1>.
- Zhang, M., Xiao, Q.T., Zhang, Z., Gao, Y.Q., Zhao, J.Y., Pu, Y.N., Wang, W., Xiao, W., Liu, S.D., Lee, X.H., 2019. Methane flux dynamics in a submerged aquatic vegetation zone in a subtropical lake. *Sci. Total Environ.* 672, 400–409. <https://doi.org/10.1016/j.scitotenv.2019.03.466>.
- Zhao, J.Y., Zhang, M., Xiao, W., Jia, L., Zhang, X.F., Wang, J., Zhang, Z., Xie, Y.H., Pu, Y.N., Liu, S.D., Feng, Z.Z., Lee, X.H., 2021. Large methane emission from freshwater aquaculture ponds revealed by long-term eddy covariance observation, 108600. *Agric. For. Meteorol.* 308–309. <https://doi.org/10.1016/j.agrformet.2021.108600>.
- Zhao, K., Zhou, Y.F., Jiang, Z.L., Hu, J., Zhang, X.S., Zhou, J., Wang, G.X., 2017. Changes of aquatic vegetation in Lake Taihu since 1960s. *J. Lake Sci.* 29, 351–362. <https://doi.org/10.18307/2017.0211> (in Chinese).
- Zhu, J.G., 2012. Hydrodynamic Mechanism of the Impact of Net Pen on the Restoration of Aquatic Vegetation in Dongtaihu Bay. (Dissertation). Graduate University of Chinese Academy of Sciences (in Chinese).